ISSN 0020-1685, Inorganic Materials, 2022, Vol. 58, No. 12, pp. 1328–1334. © Pleiades Publishing, Ltd., 2022.
Russian Text © The Author(s), 2022, published in Neorganicheskie Materialy, 2022, Vol. 58, No. 12, pp. 1377–1382.

Preparation, Microstructure, and Dielectric and Ferroelectric Properties of Modified $(1 - x)(K_{0.5}Na_{0.5})NbO_3{\cdot}xLiNbO_3$ Ceramics

E. D. Politova[a, *], G. M. Kaleva[a], A. V. Mosunov[b], S. Yu. Stefanovich[b], E. V. Klyukina[c], E. A. Bespalova[c], A. V. Lopatin[c], N. M. Metal'nikov[c], M. E. Saprykin[c], A. B. Loginov[b], I. V. Orazov[d], and B. A. Loginov[d]

[a] *Semenov Federal Research Center for Chemical Physics, Russian Academy of Sciences, Moscow, 119991 Russia*

[b] *Moscow State University, Moscow, 119991 Russia*

[c] *Sirius Education Center, Sochi, 354349 Russia*

[d] *Moscow Institute of Electronic Technology (National Research University), Zelenograd, Moscow, 124498 Russia*

**e-mail: politova@nifhi.ru*

Received April 15, 2022; revised June 14, 2022; accepted June 15, 2022

Abstract—Single-phase $(1 - x)(K_{0.5}Na_{0.5})NbO_3{\cdot}xLiNbO_3$ (KNN–LN) perovskite-structure ceramic materials with $x = 0$–0.10 modified with CuO and KCl additions have been prepared by solid-state synthesis, and their phase composition, structure, microstructure, and dielectric and ferroelectric properties have been studied. Increasing the percentage of lithium niobate has been shown to increase their Curie temperature and lower the temperature of their polymorphic phase transition, which is accompanied by a decrease in perovskite cell parameters, in accord with the ionic radii of the A-site cations. The $x = 0.2$ material has been found to have an increased room-temperature dielectric permittivity, which correlates with the observed increase in spontaneous polarization, as evidenced by laser radiation second harmonic generation intensity measurements.

Keywords: potassium sodium niobate, ceramics, perovskite structure, microstructure, ferroelectric, dielectric properties

DOI: 10.1134/S0020168522110139

INTRODUCTION

Because of the high toxicity of lead, in the past decade there has been considerable research interest in lead-free piezoelectric and other materials [1–10]. The most promising lead-free materials include oxide materials based on orthorhombic potassium sodium niobate, $(K,Na)NbO_3$ (KNN) [11–15]. One strategy for reaching good functional parameters is to vary the composition of KNN so as to bring its orthorhombic (O) to tetragonal (T) phase transition to near room temperature.

A serious drawback to such materials, responsible for the poor reproducibility of their functional properties, is that high-density, single-phase materials are difficult to prepare because of the volatility of the alkali metals at high sintering temperatures [12, 15]. In connection with this, a search for new KNN-based solid solutions and the use of low-melting-point additives capable of activating the sintering process are topical issues [8].

The purpose of this work was to study the structure, microstructure, and dielectric and ferroelectric properties of $[(K_{0.5}Na_{0.5})_{1-x}Li_x]NbO_3$ (KNN–LN) ceramics with $x = 0$, 0.02, 0.04, 0.05, 0.06, 0.07, 0.08, 0.09, and 0.10, further modified with KCl and CuO low-melting-point additives.

EXPERIMENTAL

$(1 - x)(K_{0.5}Na_{0.5})NbO_3{\cdot}xLiNbO_3$ ($x = 0$–0.10) ceramic samples without additives and containing KCl (2.5 wt %) and CuO (1 wt %) were prepared by solid-state synthesis, which included two firing steps at $T_1 =$ 900–1070 K (6 h) and $T_2 =$ 1320–1370 K (2–10 h). The starting materials used were the K_2CO_3, Na_2CO_3, and Li_2CO_3 carbonates (analytical grade), the Nb_2O_5 and CuO oxides (extrapure grade), and the KCl chloride (pure grade). Appropriate mixtures were homogenized in ethanol, pressed into disks 10 mm in diameter and 1 mm in thickness, and fired at temperatures T_1 and T_2 with intermediate grinding.

The phase composition and structural parameters of the samples were determined by X-ray diffraction (DRON-3M diffractometer, CuK_α radiation) at room temperature.

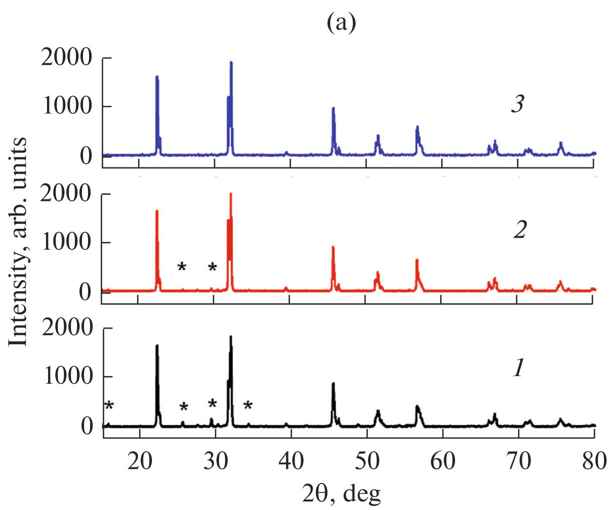

Fig. 1. X-ray diffraction patterns of (a) the $x = 0.06$ KNN–LN samples modified with 2.5 wt % KCl and fired at $T_1 = 900$ K (6 h) and T_2 = (*1*) 1360 K (2 h), (*2*) 1370 K (4 h), and (*3*) 1370 K (8 h) and (b) the KNN–LN samples with x = (*1*) 0, (*2*) 0.06, and (*3*) 0.10 prepared at $T_2 = 1320$ K (10 h).

Their microstructure was examined by atomic force microscopy on an SMM-2000 scanning probe microscope (Proton Works, Zelenograd, Russia) using MSNL silicon nitride cantilever probes (Bruker, the United States) with a tip radius (determining the resolving power of the instrument) of 2 nm (horizontal and vertical resolving powers of 1 and 0.2 nm, respectively) [16–18]. To evaluate the average grain size S of the samples (up to 2–3 μm) and their mean surface roughness R_a according to the ISO 4287 international standard, we obtained micrographs of regions (8.632–9.151) × (1.153–1.786) μm in dimensions. In addition, some of the samples were exposed to an argon plasma in an MAG-5 vacuum plasma system (manufactured at the Proton Works, Zelenograd, Russia) (argon pressure, 0.012 mbar; field strength in the plasma, 120 V/mm; ion current density, 110 mA/cm^2; exposure of the samples to the plasma for 20 s).

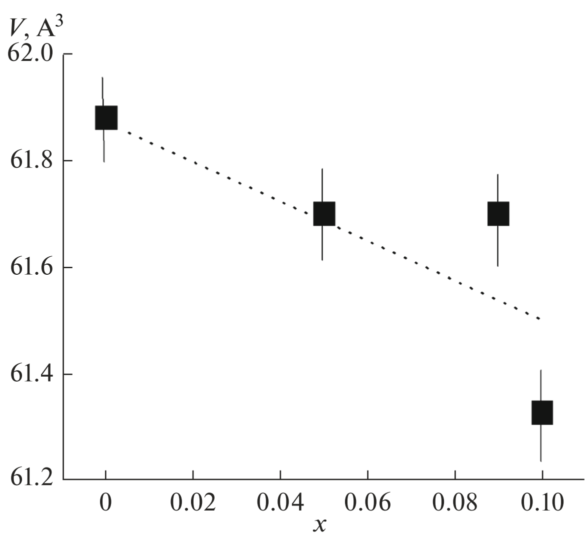

Fig. 2. Composition dependence of the unit-cell volume for the KNN–LN samples with $x = 0$, 0.05, 0.09, and 0.10.

Spontaneous polarization of the samples was estimated using second harmonic generation (SHG) of laser radiation (Nd:YAG laser, $\lambda = 1.064$ μm), whose measured signal, $q = I_{2\omega}/I_{2\omega}(SiO_2)$, was proportional to the square of spontaneous polarization P_s: $q \sim P_s^2$.

The dielectric properties of the ceramics were studied by dielectric spectroscopy (Agilent 4284 A meter, 1 V) at temperatures from 300 to 1000 K and frequencies from 100 Hz to 1 MHz.

RESULTS AND DISCUSSION

According to X-ray diffraction data, single-phase KNN–LN samples with the perovskite structure were obtained by two-step firing at $T_2 = 1320$ K (10 h), and single-phase KCl-modified samples were obtained at $T_2 = 1370$ K (8 h) (Fig. 1).

The samples had an orthorhombic structure. Figure 1b shows partial X-ray diffraction patterns of the samples, which demonstrate a sequential shift of diffraction peaks with $h^2 + k^2 + l^2 = 4$ to larger angles. This attests to a decrease in unit-cell parameters as a result of Li^+ (smaller cation) substitution for Na^+ and K^+ cations (Na^+, 1.39 Å; K^+, 1.64 Å; Li^+, 0.92 Å) (Fig. 2).

The microstructure of the modified ceramics was examined by atomic force microscopy. The surface of

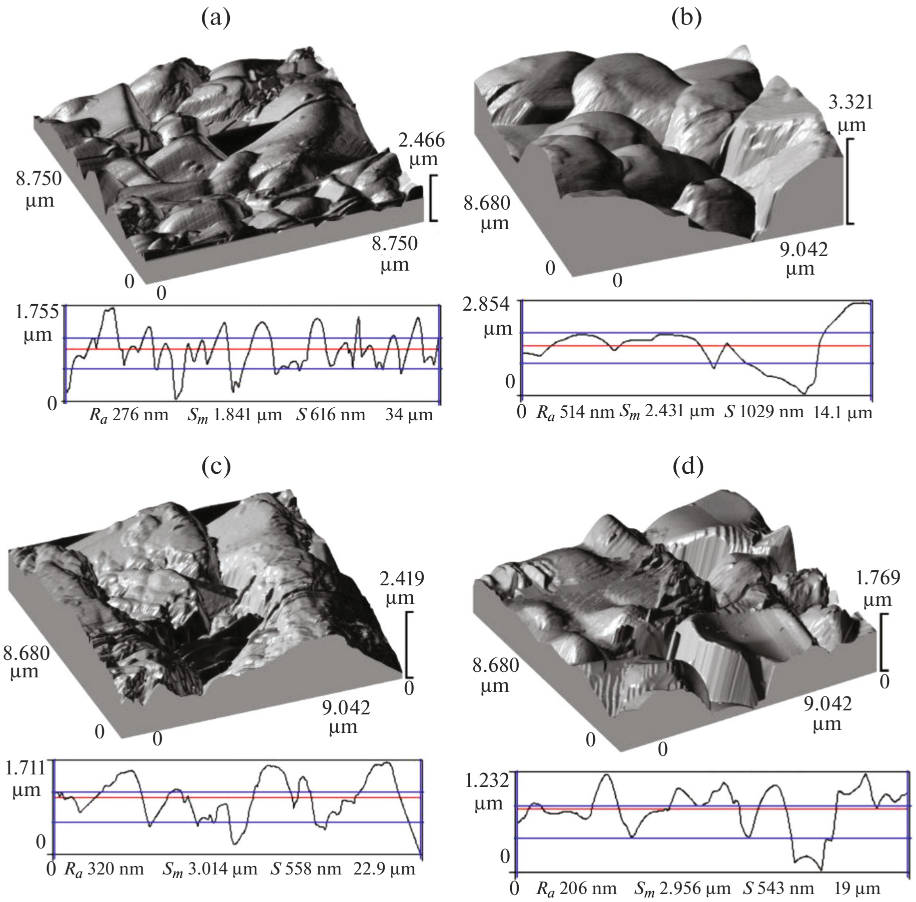

Fig. 3. Microstructure of the surface of the (a) plasma-treated CuO-modified and (b–d) KCl-modified KNN–LN samples: x = (a, b) 0, (c) 0.02, and (d) 0.05.

the samples had a uniform microstructure with a dense packing of isometric grains, which had an oval shape and an average size of ~2–3 µm and consisted of subgrains ranging in size from 400 to 1000 nm (Figs. 3, 4). In the case of modification with Cu^{2+} cations, there is a tendency for the average grain and subgrain sizes in the ceramics to decrease, which is consistent with the observed diffraction peak broadening.

For each surface topography scan, we calculated the following roughness parameters: mean roughness value (R_a), average grain size (S_m), and average size of subgrains (nanograins) forming the grains (S). To this end, we used software supplied with the SMM-2000 microscope and followed the ISO 1302 international standard (R_a is the average of the vertical displacements Z_i of all points from the mean line of the roughness profile, S_m is the average of the horizontal spacings S_{m1} and S_{m2} between intersections of ascending profile portions with the mean line, and S is the average of the horizontal spacings S_1 and S_2 between peaks of the profile) (Fig. 5).

Some of the samples were exposed to a plasma (ion flow) after removing their surface layer. The stability of the ceramics turned out to be several orders of magnitude higher than that of various metals and graphene, and the average etch rate of their surface was several orders of magnitude slower. Note that etching produced steps on the ceramic surface; that is, etching occurred only after the surface layer had flaked off (threshold effect), and some time was needed for the next layer of grains to be removed by etching. The reason for this is that, during plasma-induced heating, the first to be etched are bridges between ceramic grains. This reduces the contact area between the grains, following which the grains are heated to high temperatures and flake off.

Dielectric measurements revealed ferroelectric phase transitions characteristic of KNN-based ceramics. The transitions showed up as dielectric permittivity peaks near the polymorphic phase transition at $T(O \rightarrow T)$ ~ 420–450 K and near the Curie tempera-

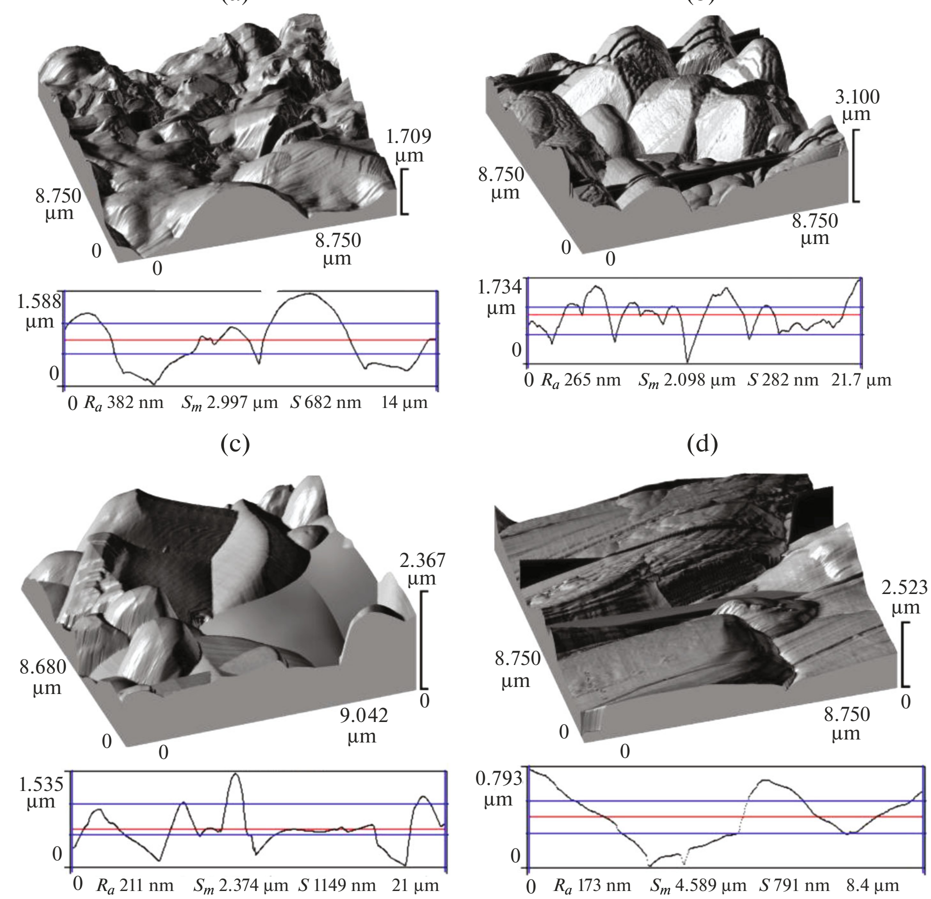

Fig. 4. Microstructure of the surface of the (b, c) CuO- and (a, d) KCl-modified KNN–LN samples: x = (a) 0.06, (c) 0.08, and (d) 0.09; (b) plasma-treated sample.

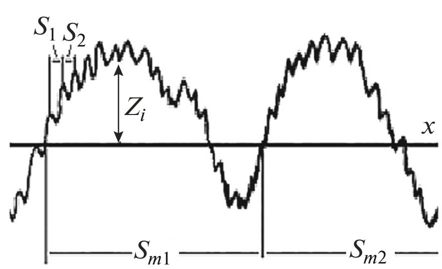

Fig. 5. Surface roughness parameters of the samples: Z_i is the vertical displacement of point i from the mean line of the roughness profile, S_{m1} and S_{m2} are the horizontal spacings between intersections of ascending profile portions with the mean line, and S_1 and S_2 are the horizontal spacings between peaks of the profile.

ture T_C ~ 650–700 K (Fig. 6). With increasing x, $T(O \rightarrow T)$ decreases, whereas T_C rises (Fig. 7).

The ferroelectric properties of the samples were confirmed by laser radiation SHG measurements. At $x = 0.02$, we observed an increased 1-kHz ε_{RT}, in accord with the SHG measurement results.

The present results are consistent with previously reported data for KNN samples modified on the A site

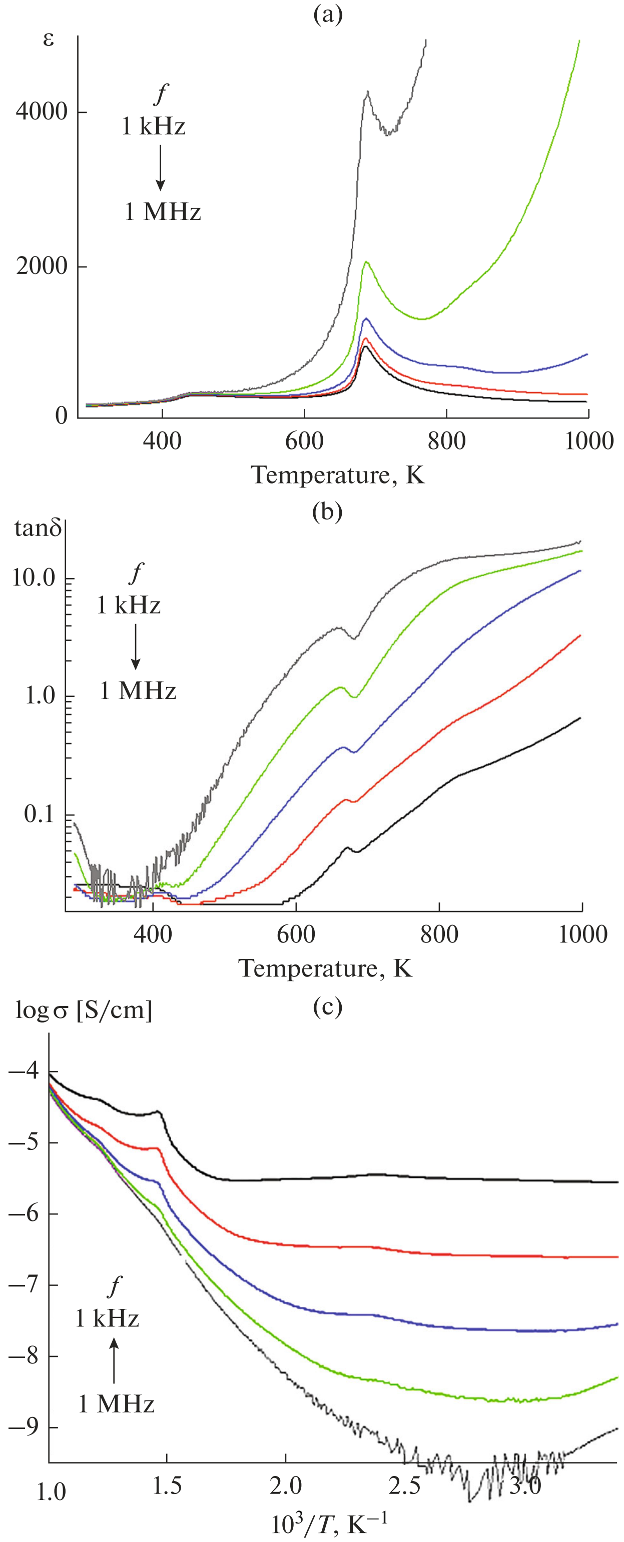

Fig. 6. Temperature dependences of dielectric permittivity ε (a) and dielectric loss tan δ (b) and Arrhenius plots of electrical conductivity σ (c) for the $x = 0.5$ KNN–LN ceramic samples at frequencies $f = 100$ Hz, 1 kHz, 10 kHz, 100 kHz, and 1 MHz.

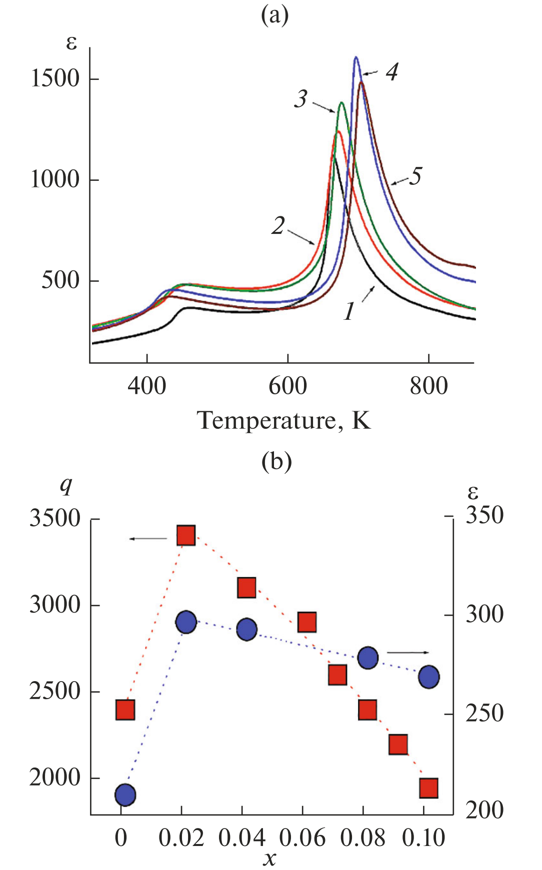

Fig. 7. (a) Temperature dependences of 1-MHz dielectric permittivity ε for the KNN–LN samples with x = (*1*) 0, (*2*) 0.02, (*3*) 0.04, (*4*) 0.08, and (*5*) 0.10 modified with 2.5 wt % KCl and fired at $T_1 = 1070$ K (6 h) and $T_2 = 1370$ K (4 h); (b) composition dependences of the SHG signal intensity $q = I_{2\omega}/I_{2\omega}(SiO_2)$ and dielectric permittivity ε at 300 K and 1 kHz for the KNN–LN samples.

[19–22] and on both the A and B sites [23, 24] with cations having a smaller ionic radius.

CONCLUSIONS

We have synthesized single-phase sodium potassium niobate-based ceramic samples, $(1 - x)(K_{0.5}Na_{0.5})NbO_3 \cdot xLiNbO_3$ (x = 0–0.10), modified with 2.5 wt % KCl and 1 wt % CuO and studied their structure, microstructure, and dielectric and ferroelectric properties. The modified samples have been shown to have a reduced unit-cell volume. Their first-order ferroelectric phase transitions near 420–450 and 650–700 K have been confirmed by dielectric spectroscopy techniques. SHG measurement results suggest that the incorporation of potassium cations into the A site of the perovskite structure enhances the ferroelectric properties of KNN ceramics.

FUNDING

This work was supported by the Russian Foundation for Basic Research (project no. 21-53-12005) and the Russian Federation Ministry of Science and Higher Education (state research target for the Semenov Federal Research Center for Chemical Physics, Russian Academy of Sciences, state registration no. 122040500071-0).

CONFLICT OF INTEREST

The authors declare that they have no conflicts of interest.

REFERENCES

1. Saito, Y., Takao, H., Tani, I., Nonoyama, T., Takatori, K., Homma, T., Nagaya, T., and Nakamura, M., Lead-free piezoceramics, *Nature,* 2004, vol. 432, pp. 84–87. https://doi.org/10.1038/nature03028
2. Maeder, M.D., Damjanovic, D., and Setter, N., Lead free piezoelectric materials, *J. Electroceram.,* 2004, vol. 13, pp. 385–392.
3. Takenaka, T., Nagata, H., and Hiruma, Y., Current developments and prospective of lead-free piezoelectric ceramics, *Jpn. J. Appl. Phys.,* 2008, vol. 47, pp. 3787–3801. https://doi.org/10.1143/JJAP.47.3787
4. Panda, P.K., Review: environmental friendly lead-free piezoelectric materials, *J. Mater. Sci.,* 2009, vol. 44, pp. 5049–5062. https://doi.org/10.1007/s10853-009-3643-0
5. Coondoo, I., Panwar, N., and Kholkin, A., Lead-free piezoelectrics: current status and perspectives, *J. Adv. Dielectr.,* 2013, vol. 3, p. 1330002. https://doi.org/10.1142/S2010135X13300028
6. Rödel, J., Webber, K.G., Dittmer, R., Wook, Jo., Kimura, M., and Damjanovic, D., Transferring lead-free piezoelectric ceramics into application, *J. Eur. Ceram. Soc.,* 2015, vol. 35 P, pp. 1659–1681. https://doi.org/10.1016/j.jeurceramsoc.2014.12.013
7. Panda, P.K. and Sahoo, B., PZT to lead free piezo ceramics: a review, *Ferroelectrics,* 2015, vol. 474, pp. 128–143. https://doi.org/10.1080/00150193.2015.997146
8. Shao, T., Du, H., Ma, H., et al., Potassium–sodium niobate based lead-free ceramics: novel electrical energy storage materials, *J. Mater. Chem. A,* 2017, vol. 5, pp. 554–563. https://doi.org/10.139/C6TA07803F
9. Rodel, J. and Li, J., Lead-free piezoceramics: status and perspectives, *MRS Bull.,* 2018, vol. 43, pp. 576–580. https://doi.org/10.1557/mrs.2018.181
10. Dongxu Li, Xiaojun Zeng, Zhipeng Li, Zong-Yang Shen, Hua Hao, Wenqin Luo, Xingcai Wang, Fusheng Song, Zhumei Wang, and Yueming Li, Progress and perspectives in dielectric energy storage ceramics, *J. Adv. Ceram.,* 2021, vol. 10, no. 4, pp. 675–703. https://doi.org/10.1007/s40145-021-0500-3
11. Suchanicz, J., Smeltere, I., Finder, A., Konieczny, K., Garbarz-Glos, B., Bujakiewicz-Koronska, R., Latas, M., Antonova, M., Sternberg, A., and Sokolowski, M., Dielectric and ferroelectric properties of lead-free NKN and NKN-based ceramics, *Ferroelectrics,* 2011, vol. 424, pp. 53–58. https://doi.org/10.1080/00150193.2011.623927
12. Cheng, L., Wang, K., Yao, F., Zhu, F., and Li, J., Composition inhomogeneity due to alkaline volatilization in Li-modified (K,Na)NbO_3 lead-free piezoceramics, *J. Am. Ceram. Soc.,* 2013, vol. 96, pp. 2693–2695. https://doi.org/10.1111/jace.12497
13. Li, J.F., Wang, K., Zhu, F.Y., Cheng, L.Q., and Yao, F.Z., (K,Na)NbO_3-based lead-free piezoceramics: fundamental aspects, processing technologies, and remaining challenges, *J. Am. Ceram. Soc.,* 2013, vol. 96, pp. 3677–3696. https://doi.org/10.1111/jace.12715
14. Wu, J.G., Xiao, D.Q., and Zhu, J.G., Potassium–sodium niobate lead-free piezoelectric materials: past, present, and future of phase boundaries, *Chem. Rev.,* 2015, vol. 115, pp. 2559–2595. https://doi.org/10.1021/cr5006809
15. Malic, B., Koruza, J., Hrescak, J., Bernard, J., Wang, K., Fisher, J., and Bencan, A., Sintering of lead-free piezoelectric sodium potassium niobate ceramics, *Materials,* 2015, vol. 12, pp. 8117–8146. https://doi.org/10.3390/ma8125449
16. Loginov, B.A., Loginov, P.B., Loginov, V.B., and Loginov, A.B., Probe microscopy: applications and recommendations on development, *Nanoindustriya,* 2019, vol. 12, no. 6, pp. 352–365. https://doi.org/10.22184/1993-8578.2019.12.6.352.364
17. Loginov, A.B., Bozhev, I.V., Bokova-Sirosh, S.N., Obraztsova, E.D., Ismagilov, R.R., Loginov, B.A., and Obraztsov, A.N., Few-layer graphene formation by carbon deposition on polycrystalline Ni surface, *Appl. Surf. Sci.,* 2019, vol. 494, pp. 1030–1035. https://doi.org/10.1016/j.apsusc.2019.07.254
18. Loginov, B.A., Some new capabilities of probe microscopy for semiconductor structure surface analysis, *Trudy XXV Mezhdunarodnogo simpoziuma "Nanofizika i nanoelektronika"* (Proc. XXV Nanophysics and Nanoelectronics Int. Symp.), Nizhny Novgorod, 2021, vol. 2, pp. 739–740.
19. Politova, E.D., Golubko, N.V., Kaleva, G.M., Mosunov, A.V., Sadovskaya, N.V., Stefanovich, S.Yu., Kiselev, D.A., Kislyuk, A.M., Chichkov, M.V., and Panda, P.K., Structure, ferroelectric and piezoelectric properties of KNN-based perovskite ceramics, *Ferroelectrics,* 2019, vol. 538 P, pp. 45–51. https://doi.org/10.1080/00150193.2019.1569984
20. Politova, E.D., Kaleva, G.M., Golubko, N.V., Mosunov, A.V., Sadovskaya, N.V., Kiselev, D.A., Kislyuk, A.M., Ilina, T.S., and Stefanovich, S.Yu., Silver niobate doped lead-free perovskite KNN ceramics, *IOP Conf. Ser.: Mater. Sci. Eng.,* 2020, vol. 848, p. 012072. https://doi.org/10.1088/1757-899X/848/1/012072
21. Politova, E.D., Kaleva, G.M., Mosunov, A.V., Stefanovich, S.Yu., Sadovskaya, N.V., Ilina, T.S., Kis-

lyuk, A.M., and Kiselev, D.A., Influence of A-site doping on properties of lead-free KNN-based perovskite ceramics, *Ferroelectrics,* 2021, vol. 575, pp. 158–166.
https://doi.org/10.1080/00150193.2021.1888239

22. Talanov, M.V., Shilkina, L.A., and Reznichenko, L.A., Synthesis and properties of $Na_{1-x}K_xNbO_3$-based solid solutions in the $CuNb_2O_6$–$NaNbO_3$–$KNbO_3$ system, *Inorg. Mater.,* 2016, vol. 52, no. 10, pp. 1063–1069.
https://doi.org/10.1134/S0020168516100186

23. Kaleva, G.M., Mosunov, A.V., Stefanovich, S.Yu., and Politova, E.D., Preparation and dielectric properties of potassium sodium niobate-based solid solutions, *Inorg. Mater.,* 2013, vol. 49, no. 8, pp. 826–833.
https://doi.org/10.1134/S0020168513080074

24. Kaleva, G.M., Politova, E.D., Mosunov, A.V., and Stefanovich, S.Yu., Phase formation, structure, and dielectric properties of modified potassium sodium niobate ceramics, *Inorg. Mater.,* 2020, vol. 56, no. 10, pp. 1072–1078.
https://doi.org/10.1134/S0020168520100076

Translated by O. Tsarev